Biophysical Chemistry 141 (2009) 41–48

Contents lists available at ScienceDirect

Biophysical Chemistry

journal homepage: http://www.elsevier.com/locate/biophyschem

Quantitative evaluation of respiration induced metabolic oscillations in erythrocytes

Bjørn Hald [a,*], Mads F. Madsen [a,1], Sune Danø [a,1], Bjørn Quistorff [a], Preben G. Sørensen [b]

[a] Department of Biomedical Sciences, University of Copenhagen, Copenhagen, Denmark
[b] Department of Chemistry, University of Copenhagen, Copenhagen, Denmark

ARTICLE INFO

Article history:
Received 22 September 2008
Received in revised form 15 December 2008
Accepted 20 December 2008
Available online 31 December 2008

Keywords:
Erythrocytes
Blood circulation
Mathematical modelling
Oscillations

ABSTRACT

The changes in the partial pressures of oxygen and carbon dioxide (P_{O_2} and P_{CO_2}) during blood circulation alter erythrocyte metabolism, hereby causing flux changes between oxygenated and deoxygenated blood. In the study we have modeled this effect by extending the comprehensive kinetic model by Mulquiney and Kuchel [P.J. Mulquiney, and P.W. Kuchel. Model of 2,3-bisphosphoglycerate metabolism in the human erythrocyte based on detailed enzyme kinetic equations: equations and parameter refinement, Biochem. J. 1999, 342, 581–596.] with a kinetic model of hemoglobin oxy-/deoxygenation transition based on an oxygen dissociation model developed by Dash and Bassingthwaighte [R. Dash, and J. Bassingthwaighte. Blood HbO_2 and $HbCO_2$ dissociation curves at varied O_2, CO_2, pH, 2,3-DPG and temperature levels, Ann. Biomed. Eng., 2004, 32(12), 1676–1693.]. The system has been studied during transitions from the arterial to the venous phases by simply forcing P_{O_2} and P_{CO_2} to follow the physiological values of venous and arterial blood. The investigations show that the system passively follows a limit cycle driven by the forced oscillations of P_{O_2} and is thus inadequately described solely by steady state consideration. The metabolic system exhibits a broad distribution of time scales. Relaxations of modes with hemoglobin and Mg^{2+} binding reactions are very fast, while modes involving glycolytic, membrane transport and 2,3-BPG shunt reactions are much slower. Incomplete slow mode relaxations during the 60 s period of the forced transitions cause significant overshoots of important fluxes and metabolite concentrations – notably ATP, 2,3-BPG, and Mg^{2+}. The overshoot phenomenon arises in consequence of a periodical forcing and is likely to be widespread in nature – warranting a special consideration for relevant systems.

1. Introduction

The erythrocyte is a simple cell in the sense that it obtains its energy and redox equivalents entirely from anaerobic metabolism of glucose through glycolysis and the pentose phosphate pathway (PPP – see list of abbreviations). Furthermore, it has no genetic material which simplifies modelling considerably. Many kinetic models have been developed that have described the intercellular dynamics focusing on the oxygenated and deoxygenated steady state concentrations. The numerically simplest way to obtain information on steady state dynamics is through modal analysis [1] (see 'Theory') in which the relaxation times for each mode of a steady state are the reciprocals of the real part of the eigenvalues of the Jacobian. There is no general method for calculation of explicit expressions for the dependence of relaxation times on kinetic parameters in many-component systems. The general trend can be illustrated by considering a simple example. In a linear irreversible chain

$$\rightarrow S_1 \xrightarrow{k_1} S_2 \xrightarrow{k_2} S_3 \cdots S_{n-1} \xrightarrow{k_{n-1}} S_n \xrightarrow{k_n}$$

the eigenvalues of the Jacobian are $-k_1, -k_2, \cdots, -k_n$ and the corresponding relaxation times are $\tau_i = 1/k_i$. In this case the largest relaxation time is quite naturally the reciprocal of the smallest rate constant. If the reactions in a

Abbreviations: Metabolites: Glc, α-D-glucose; G6P, α-D-glucose-6-phosphate; FBP, β-D-fructose 1,6-bisphosphate; 1,3-BPG, 1,3-biphosphoglycerate; 2,3-BPG, 2,3-biphosphoglycerate; PEP, phosphoenolpyruvate; Pyr, (S)-pyruvate; Lac, L-lactate; GSH, Glutathione; NADH, Nicotinamide adenine dinucleotide (reduced form); NADPH, Nicotinamide adenine dinucleotide phosphate (reduced form); P_i, inorganic phosphate; Hb_d, deoxy-hemoglobin; Hb_o, oxy-hemoglobin; *Enzymes*: HK, hexokinase (EC 2.7.1.1); PGI, glucose-6-phosphate isomerase (EC 5.3.1.9); PFK, 6-phosphofructo kinase (EC 2.7.1.11); ALD, fructose-bisphosphate aldolase (EC 4.1.2.13); TPI, triose phosphate isomerase (EC 5.3.1.1); GAPDH, glyceraldehyde 3-phosphate dehydrogenase (phosphorylating) (EC 1.2.1.12); BPGSP, bisphosphoglycerate synthase/phosphatase (EC 5.4.2.4 and EC 3.1.3.13); BPGSP7, the 2,3-BPG producing elementary reaction in the shunt; PGK, phosphoglycerate kinase (EC 2.7.2.3); PGM, phosphoglycerate mutase (EC 5.4.2.1); ENO, phosphopyruvate hydratase (EC 4.2.1.11); PK, pyruvate kinase (EC 2.7.1.40); LDH, L-lactate dehydrogenase (EC 1.1.1.27); G6PDH, glucose 6-phosphate dehydrogenase (EC 1.1.1.49); Ru5PE, ribulose-5-phosphate epimerase (EC 5.1.3.1); TK, transketolase (EC 2.2.1.1); AK, adenylate kinase (EC 2.7.4.3); *Lumped enzymatic reactions*: ATPase, non-glycolytic energy consumption; oxNADH, reducing processes requiring NADH; PyrTR, pyruvate transport; LacTR, lactate transport; PhosTR, inorganic phosphate transport; *Miscellaneous*: cdB3, cytoplasmatic domain of Band3; MCA, Metabolic Control Analysis; P_{O_2}, partial pressure of O_2; PPP, pentose phosphate pathway; SI, Supplementary information.

* Corresponding author. Department of Biomedical Sciences, University of Copenhagen, Blegdamsvej 3, 2200 Copenhagen, Denmark. Tel.: +45 3532 7403; fax: +45 3532 7070.
E-mail address: bjornhald@gmail.com (B. Hald).
[1] Present address: Topsoe Fuel Cell, Lyngby, Denmark.

0301-4622/$ – see front matter © 2008 Elsevier B.V. All rights reserved.
doi:10.1016/j.bpc.2008.12.008

chain are reversible the width of the relaxation time distribution increases. Furthermore, feedback over distant parts of the network may considerably increase the relaxation times. In the Supplementary material (SI, Section 1.1) the Yates–Pardee model is used to exemplify changes in time scale distribution to the point where the system become unstable and the largest relaxation time becomes infinite. Erythrocyte metabolism contains several linear chains with reversible reactions and feedback, and it is not surprising that models of this system have extremely slow modes with relaxation times of several hours as shown by [2].

Compared with the period of circulation at rest of around 60 s it is clear that a complete relaxation to steady state may not occur if the slow modes are excited. Fast modes corresponding to small relaxation times may follow environmental variations accurately while slow modes never relax completely to the current steady state. Consequently, to describe physiological behavior the temporal behavior of the bloodstream must be taken into account.

Experimental evidence suggests that steady state glycolytic flux is higher in deoxygenated blood compared to oxygenated blood *in vitro* [3–7], whereas the opposite to a lesser extent is true for the PPP [3]. The flux changes have been hypothesized to satisfy the demand for NADPH under oxygenated conditions and replenish the ATP stores under deoxygenated conditions [3,8]. The findings imply that dynamic changes take place across pulmonary and peripheral tissues where O_2 and CO_2 rapidly exchange. In this study we have extended the steady state model of human erythrocyte metabolism developed by Mulquiney and Kuchel [9,10]. Specifically, our extended model includes mathematical descriptions of: 1) The transition kinetics of Hb, building on previous work by Dash and Bassingthwaighte [11] and 2) The oscillatory concentrations of O_2 and CO_2 in erythrocytes, forced by the repeated passage of the erythrocytes through the arterial and venous compartments of the circulatory system (see 'Methods').

We estimate the changes in erythrocyte metabolism upon forced oscillatory gas exchanges. Besides glycolytic flux changes, the forcing also causes significant overshoots of a number of important metabolites – notably ATP, 2,3-BPG, and Mg^{2+} – which may have physiological consequences for erythrocytes.

The study exemplifies the use of modelling to disclose an emergent property of a biochemical network, here the overshoot-phenomena observed from simulations of the present model.

2. Theory

The kinetic model of erythrocyte metabolism in this study encompasses 63 metabolites and 60 reactions. A schematic drawing of the extended model is shown in Fig. 1. The red species are able to bind Hb. Species able to cross the membrane are shown in blue. Extracellular Glc, Lac, Pyr and P_i are treated as constants, whereas P_{O_2} and P_{CO_2} are forced. The model encompasses descriptions of glycolysis, PPP, 2,3-BPG shunt, Hb and Mg^{2+} binding reactions, and the Hb oxy/deoxy transitions as well as the forcing of P_{O_2} and P_{CO_2}. The complete set of reaction rate expressions can be found in the 'Supplementary Information' (SI). Key parameters and initial conditions of the model are given in Tables S3 and S4 in the SI.

The model of erythrocyte metabolism by Mulquiney and Kuchel [9] was chosen because it, to our opinion, is the most comprehensive model with respect to 2,3-BPG metabolism and Hb and Mg^{2+} metabolite binding reactions. A huge level of detail is needed in order to assess the possible effects of respiration on the core metabolism. The most important allosteric regulations are the 2,3-BPG and ATP inhibition and AMP activation of PFK. Table S5 in the SI presents the most important allosteric effectors of HK, PFK, ALD, and PK.

2.1. Modal analysis

Modal analysis of steady states is a general method to get information on the time scales of a metabolic network. The time scales are the characteristic times for metabolic processes to reach completion. The relevant process in this study is the relaxation of an arbitrary state to a stationary state. If the characteristic time for this process is always smaller than the circulation time of the blood the state of the system will almost always be close to one of the stationary states. For initial states close to the stationary state the characteristic times are called the relaxation times. They can be calculated from the eigenvalues of the Jacobian matrix evaluated at the steady state. The Jacobian matrix is defined as

$$J = N\frac{\partial \boldsymbol{v}}{\partial \boldsymbol{S}} \tag{1}$$

where **N** is the stoichiometric matrix, and $\boldsymbol{v}$ is a vector containing all rates as elements, and $\boldsymbol{S}$ is the vector of metabolite concentrations. The eigenvalues of the Jacobian are determined by diagonalizing the Jacobian at the steady state (in this study *Mathematica* (Wolfram Inc.) was used). The relaxation times are defined by

$$\tau_i = \frac{1}{|\mathrm{Re}(\lambda_i)|} \quad i = 1, 2, 3, \ldots, n \tag{2}$$

where λ_i are the corresponding eigenvalues of the Jacobian [1].

The modes are the eigenvectors $\boldsymbol{e}_i$ of the Jacobian. They can be considered as a basis of n orthogonal vectors, pointing out the directions in the space of metabolite concentrations along which the system relaxes back to the steady state with the relaxation times τ_i. The reactions involved in this relaxation can be determined by transforming the eigenvectors of the Jacobian from concentration space to reaction space which is a space with reaction extents as coordinates. This is done most easily by calculating derivatives of reaction rates with respect to the metabolite concentrations (i.e. calculating the unnormalized elasticity-matrix of Metabolic Control Analysis (MCA)), and multiplying this matrix with the eigenvectors of the Jacobian. The transformed eigenvectors are the columns of

$$\frac{\partial \boldsymbol{v}}{\partial \boldsymbol{S}} \cdot \boldsymbol{W} \tag{3}$$

where $\boldsymbol{W}$ contains the eigenvectors of the Jacobian as columns. Transformations of this type are used in Table 2.

As the eigenvectors constitute a basis, any vector, $\boldsymbol{u}$, in the metabolite space can be written as a linear combination of the eigenvectors $\boldsymbol{u} = \Sigma\, c_i \boldsymbol{e}_i$. The coefficients, c_i, may be calculated by projecting $\boldsymbol{u}$ onto the eigenvectors. A coefficient value c_i measures the extent to which the relaxation of $\boldsymbol{u}$ can be ascribed the individual relaxation mode. As the Jacobian may be an unsymmetrical matrix – a usual property of Jacobians of open chemical systems – projections on the right eigenvectors of the Jacobian have to be performed using left eigenvectors, denoted $\boldsymbol{e}^i$, $i = 1, 2, \ldots, n$ [12]:

$$\boldsymbol{e}^i \boldsymbol{u} = c_i$$

This procedure is utilized in Table 3.

3. Methods

The extensions to the core model by Mulquiney and Kuchel [9] include the Hb transition reaction, $Hb_d \rightleftharpoons Hb_o$ and a model that can force concentrations of selected species during blood circulation.

3.1. Hemoglobin transition

The rate equation of the Hb (oxy–deoxy) transition is based on the following three major assumptions: First, the reaction kinetics is fast compared with the frequency of circulation. Second, it is assumed that

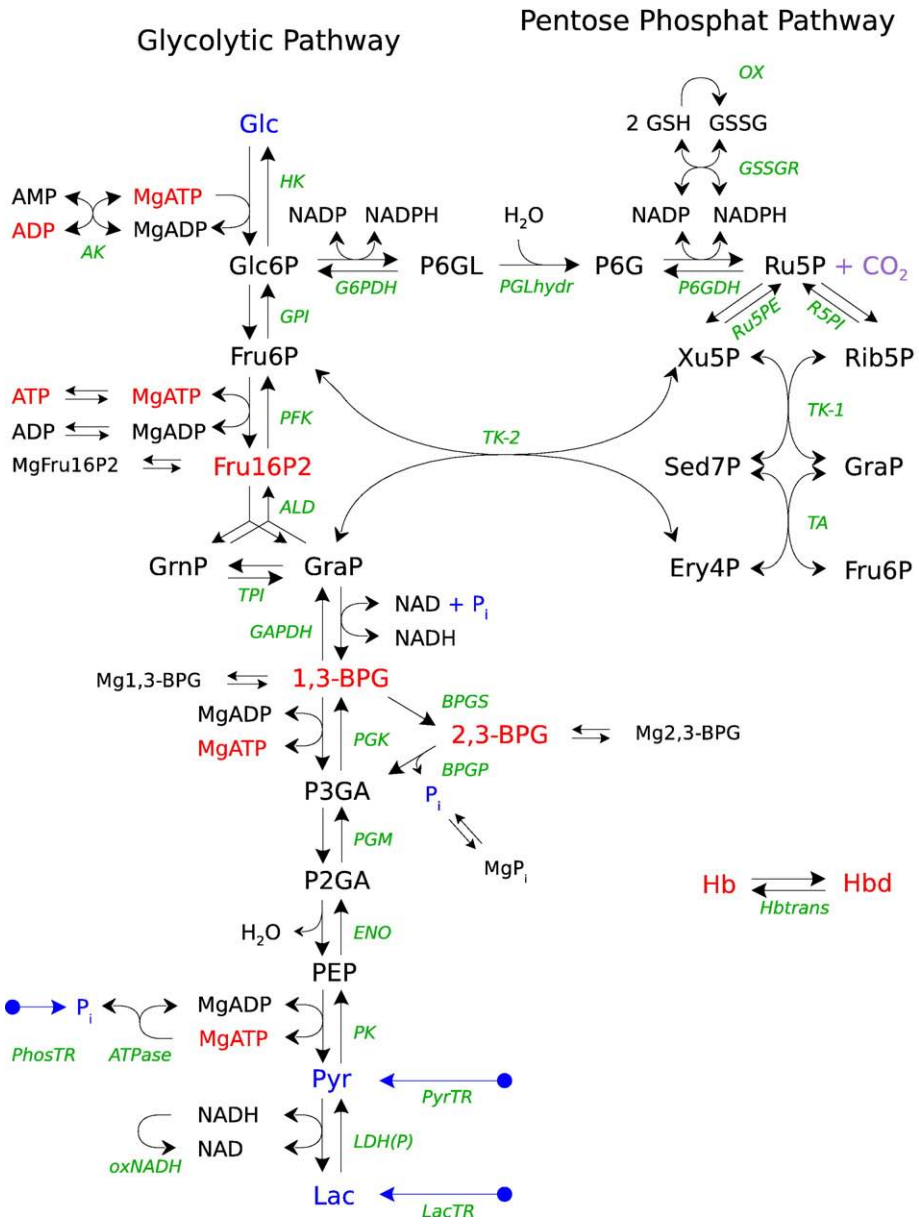

Fig. 1. Core metabolism of human erythrocytes. The figure shows the reactions of erythrocyte metabolism considered in the model. The red species are metabolites capable of binding to Hb. The blue species are species also present extracellularly and are transported across the cell membrane. CO_2 is drawn purple as the concentration of CO_2 is forced in the model. (Abbreviations can be found in the SI).

Hb only undergoes transition between the T and R states. Fully deoxygenated Hb is thus equivalent with the T state and vice versa for the R state – no intermediaries are accounted for. Third, only Hb with no heterotropic ligands attached is able to undergo a transition in the model description.

With these assumptions the rate equations can be approximated by:

$$v_{forward} = k \cdot [Hb_d] \cdot K_{Hb}$$

$$v_{backward} = k \cdot [Hb_o]$$

where the equilibrium constant K_{Hb} is a function of P_{O_2}, 2,3-BPG, pH, P_{CO_2}, and temperature (see [11] and in the SI). The scaling constant k is set to 10^5 to enforce fast transition (changing the k-value from 10^2 to 10^9 does not change the behavior of the system). Derivation of the rate equation is found in Section 2 in the SI.

3.2. Model description of blood circulation

The modelling of the blood circulation is based on the assumption that the bloodstream consists of just four compartments, namely: the arteries (between the left ventricle and the organs), the organ capillaries, the veins (between the organs and the right ventricle), and the lung capillaries (between the right and left ventricle of the heart). The chemical composition of blood experienced by an erythrocyte especially P_{O_2} and P_{CO_2} oscillates in time as it passes through these four compartments at a constant velocity. This forces transitions between oxy- and deoxy-Hb to occur in the organ capillaries and in the capillaries of the lungs.

The model of oscillatory forcing employs a 'step-like' function (see Section 3 in the SI) in which the phase and amplitude of a forced species can be arbitrarily chosen. The forcing of P_{O_2} and P_{CO_2} can be seen in Fig. 2.

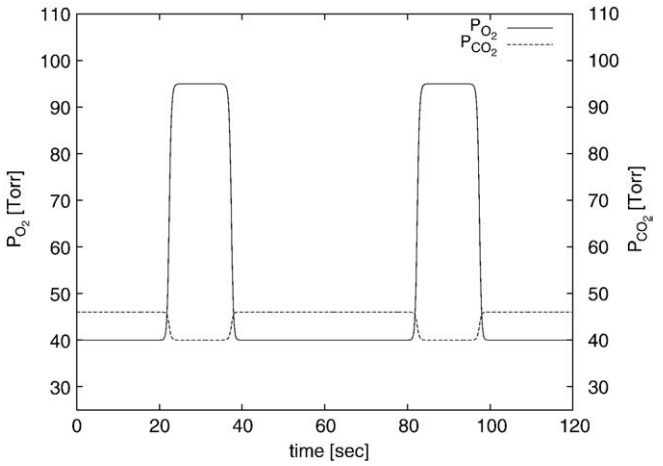

Fig. 2. Forced oscillations of P_{O_2} (solid line) and P_{CO_2} (dashed line). Two periods of circulation is shown, i.e. 120 s. The length of the venous, arterial and capillary phases are about 42.5, 13.5 and 2×2.0 s, respectively [45].

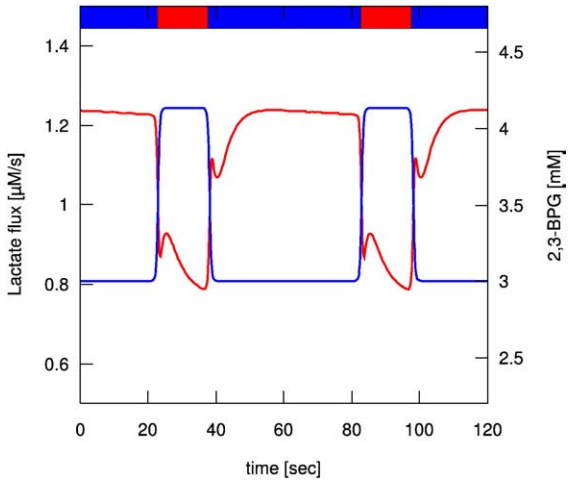

Fig. 3. Limit cycle oscillations of lactate flux (red curve) and free 2,3-BPG concentration (blue curve) as functions of time. The bar at the top of the figure indicates the arterial (red) and venous (blue) phases. The period of [2,3-BPG] oscillations follows the period of forced oxygen strictly.

3.3. pH considerations

Arterio-venous variations in pH are also known to occur in the blood and differences are dramatically enhanced upon physical exercise [13]. However, at rest the intracellular compartment of erythrocytes is remarkably stable against arterio-venous pH variations in the blood, i.e. intracellular pH only changes ≈0.05 units in the course of circulation due to the high buffer capacity of Hb and the Haldane effect [14–16]. Consequently, the pH influence on metabolism at rest is very limited. As inclusion would cause considerable additional computational load and questionable reaction kinetics, pH variations are neglected in the model.

3.4. Integration method

The set of coupled ODEs was integrated forward in time using CVODE [17] for stiff problems (Backward Differentiation Formulas – version from Sept. 1994) with an absolute $\epsilon_a = 10^{-18}$ and a relative $\epsilon_r = 10^{-10}$. CVODE is part of a free suite of numerical integrators collectively known as *Sundials* and can be downloaded at: www.llnl.gov/CASC/sundials/.

Typical simulations were completed within a minute on a standard dual core PC.

4. Results

Simulating the erythrocyte system circulating periodically between the arterial and venous compartments shows that the intracellular metabolite concentrations oscillate as well, i.e. the system passively follows a limit cycle driven by the forced oscillations of O_2 and CO_2 tensions. Fig. 3 illustrates the oscillations of lactate flux and the free 2,3-BPG concentration. Generally, the metabolite concentrations follow the steady state values corresponding to changes in O_2 and CO_2. Yet, this is not the case for many reaction fluxes as well as concentrations of Hb, Mg^{2+} (free or metabolite bound), 2,3-BPG, ATP and ADP as shown below.

By inserting parameter values characteristic of the arterial and venous compartments, respectively, the system was also allowed to attain either arterial or venous steady state. Comparison of the arterial and venous steady states revealed that the sets of concentrations and fluxes are highly similar, as summarized in Tables S6 and S7 in the SI. (For comparison, data for the arterial steady state predicted by the model by Mulquiney and Kuchel and previously published values for the corresponding metabolites are also given in Table S8.)

The main result of the study is that the arterio-venous (AV) ratios of a number of important reaction fluxes and metabolite concentrations in the forced system of circulating erythrocytes differ significantly from the corresponding ratios for steady state simulations. Nonetheless, most intermediary metabolites of the glycolytic and PPP pathways are fairly constant. Table 1 shows ratios between important metabolite concentrations and reaction fluxes, respectively, calculated between a) the late arterial and late venous phase on the limit cycle and b) the arterial and venous steady states (Hb species are left out because of their trivial oxy–deoxy ratios). For metabolites it is readily seen that limit cycle to steady state ratios of 2,3-BPG, ATP, FBP, Mg^{2+} and Mg^{2+} bound species are of significance (ratios between 15 and 40%). For reaction fluxes the ratios through most of the glycolytic pathway, 2,3-BPG shunt and membrane transports are even greater (differences between 50 and 700%. Differences are also seen for AK, Mg^{2+} and Hb binding reactions but here the steady state fluxes are zero). Transport of Lac, Pyr, and P_i can explain the smaller ratios with respect to metabolites.

These AV ratios between the limit cycle and steady states are called overshoots in the following. Overshoot examples are illustrated in Fig. 4. The dynamics leading to the observed behavior is analyzed through the use of relaxation modes.

4.1. Relaxation modes

Calculation of the relaxation modes of the steady states revealed that the 54 relaxation modes (there are 9 conserved chemical moieties

Table 1
Overshoots of selected metabolite concentrations (left) and reaction rates (right)

Metabolite	L.C.	St.st.	Flux	L.C.	St.st.
G6P	1.03	0.98	HK	0.93	0.97
Mg	0.84	0.99	G6PDH	1.01	1.00
Mg2,3-BPG	1.15	1.02	PFK	0.46	0.96
MgATP	0.96	0.96	LDH	0.68	0.97
2,3-BPG	1.38	1.03	BPGSP7	−1.76	NA
ADP	1.04	0.93	oxNADH	0.94	0.99
ATP	1.14	0.97	AK	−0.17	NA
AMP	0.94	0.90	*mg23bpg*	−0.19	NA
FBP	0.75	1.01	Hb_o23BPG	47.96	NA
NADH	0.94	0.99	PyrTR	0.12	1.01

Arterio-venous ratios are calculated both on the limit cycle (L.C.) and between steady states (St.st.). Values representing the arterial and venous phases on the limit cycle are taken to be the last time point before a perturbation (capillary traversal) occurs. BPGSP7: The 2,3-BPG producing reaction in the 2,3-BPG shunt. oxNADH: unspecified reducing processes requiring NADH. NA: Not Applicable – steady state flux zero.

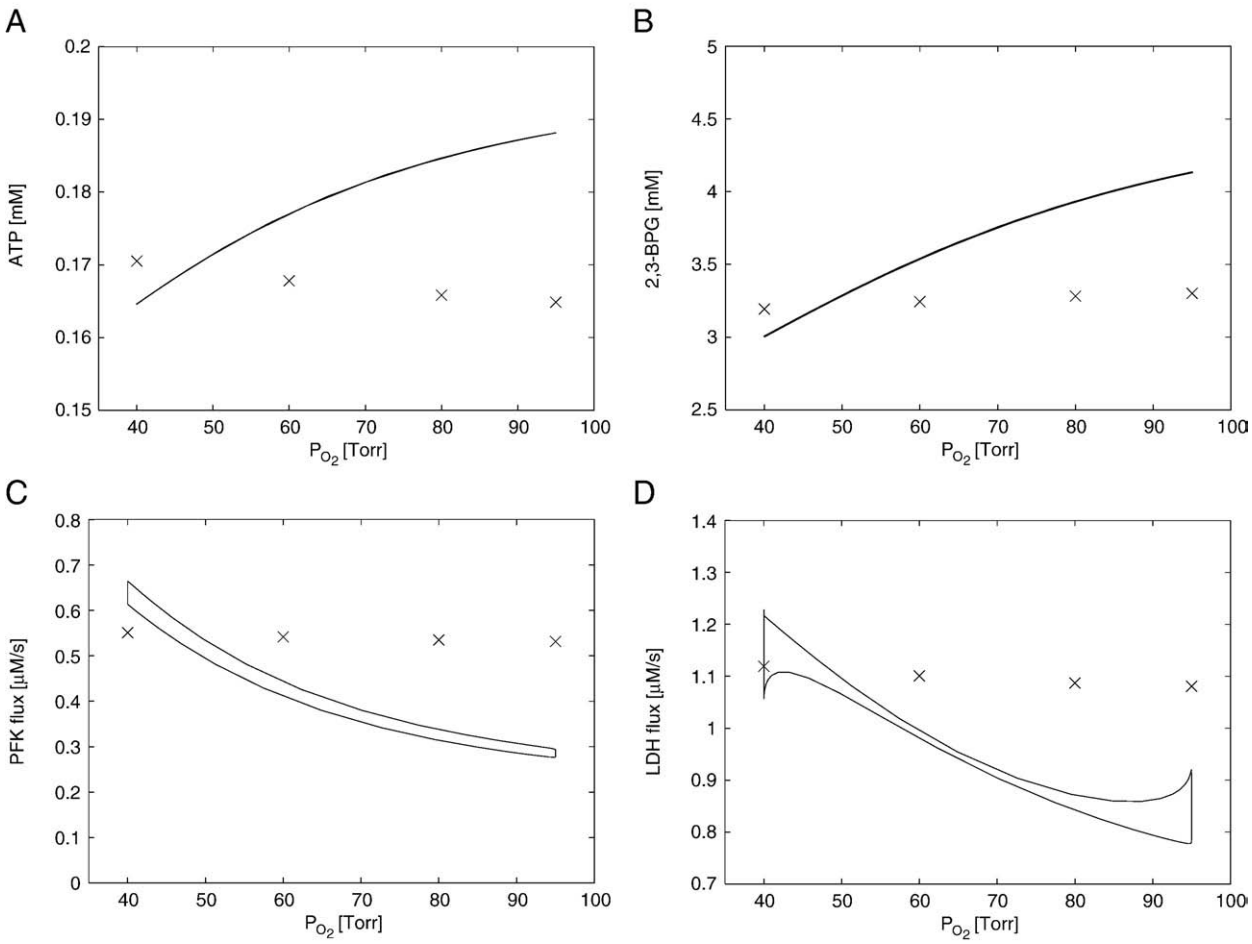

Fig. 4. Overshoot phenomenon in ATP (A) and 2,3-BPG (B) concentration and PFK (C) and LDH (D) fluxes. The figure compares the concentration or flux on the forced limit cycles (curves) to the steady states (crosses) at a forcing amplitude of 40 to 95 Torr. The crosses mark the steady state concentrations 40, 60, 80, and 95 Torr, respectively.

in the model) of the arterial steady state are highly similar to the modes of the venous steady state (data not shown). Table 2 presents a short overview of the modes where the relaxation times and most involved reactions have been grouped together (more detail can be found in the SI). It can be seen that Hb and Mg^{2+} binding reactions are exclusively present in the very fast modes, while glycolytic, 2,3-BPG shunt, and transport reactions are components of the slow modes. These findings agree with previous models of erythrocyte metabolism (e.g. [2,9]).

4.2. The forced system

The period of blood circulation at rest is approximately 60 s [13]. Hence, the time window provided by the circulatory forcing is too small to allow complete relaxation of the system in the arterial or venous steady state. It was tested that no instabilities were introduced on the limit cycle by the forced oscillations, i.e. no eigenvalue becomes positive (data not shown), and it must be concluded that the limit cycle is a passive response to the P_{O_2} oscillations that primarily drives the system. P_{CO_2} oscillations in the physiological range of 40–46 Torr alone could not produce significant flux oscillations in the system. Consequently, shifting the Hb transition equilibrium through P_{O_2} perturbs the system through the Hb-metabolite binding reactions, hereby causing a change of the attractor location in metabolite space.

To estimate which modes would be excited and to what extent, if infinite relaxation after a perturbation was allowed, concentration differences between a) the early arterial phase of the limit cycle and arterial steady state, and b) the early venous phase of the limit cycle and venous steady state were projected onto arterial steady state eigenvectors. The results are displayed in Table 3. For both projections mode no.54 (the very slow, 2,3-BPG producing mode) is the preponderant mode that cannot achieve relaxation in the time frame given by the respiratory forcing.

Table 2
Overview of relaxation modes of the steady states

Mode nos.	$\frac{1}{\lvert Re(\lambda_i)\rvert}$ time	Largest components
1–24	<2 ms	Mostly Hb and Mg^{2+} binding reactions
25–39	<1 s	Mostly PPP reactions
40–44	<10 s	Glycolytic, PPP, Hb and Mg^{2+} binding reactions
45–50	<4 m	Glycolysis, 2,3-BPG shunt and Lac, Pyr and P_i transport
51–54	8 m–5 h	2,3–BPG shunt, glycolysis and Lac, Pyr and P_i transport

The relaxation back to steady state upon a perturbation can be systematically presented through eigenmode analysis of the steady state. In the 'Largest component'-columns, reactions which have the largest components of the reaction space eigenvectors corresponding to the indicated relaxations times are shown.

4.3. System dynamics

Because of the relative closeness to the arterial and venous steady states, the overshoots displayed by the forced system compared to the steady states can be explained to a large part in terms of the eigenvectors and associated eigenvalues of the Jacobian. That is, the exact geometry of the "excited" eigenvectors in the phase plane and the magnitude of the corresponding eigenvalues coupled with the amplitude and "effectiveness" (flux control) of the forced parameters.

As an illustrative example we consider a two-dimensional system for which two relaxation modes – one fast and one slow – relax towards steady state. As illustrated in Fig. 5, periodic changes of an

Table 3
Full relaxation to steady state after capillary traversal (in the forced system) requires mostly relaxation of mode no.54

(a) Arterial projection		(b) Venous projection	
Mode	Coef	Mode	Coef
54	71.2%	54	50.1%
47	4.5%	6	9.1%
46	4.5%	2	6.0%
45	4.0%	7	5.8%
6	2.8%	45	4.3%
51	2.7%	46/47	4.0%
Sum of coefficients relative to sum of coefficients from the venous projection			
	3.5		1.0

The table shows the normalized coefficients ($coef_i/\Sigma coef_i$) from projections of concentration differences between: (a) the early arterial phase of the limit cycle and the arterial steady state and (b) early venous phase and venous steady state. The total sum from the arterial projection is 3.5 times larger than the venous projection.

external parameter translocates the steady state, where the magnitude of translocation depends on the amplitude of oscillations and flux control of the parameter. Nevertheless, the properties of the relaxation modes may remain largely unaltered (at any given time-point only one steady state is present. The two steady states shown represent the steady state at the two different values of the external parameter). The "fast" eigenvector determines the initial direction of relaxation followed by slow relaxation along the direction of the "slow" eigenvector. From Fig. 5 it is clear that the angle between the eigenvectors, the separation of time scales, the frequency of periodic transitions, and the distance between the steady state locations determines the extent of overshoots for some species on the limit cycle. For some species, ratios are larger on the limit cycle compared with ratios between the steady state locations.

The data in Tables 2 and 3 show that the slow 2,3-BPG producing reaction modes combined with fast Hb and Mg^{2+} binding reaction modes provide the basis for the observed dynamics in the high dimensional case of erythrocyte metabolism. The slow 2,3-BPG producing reaction mode are excited but cannot relax in the timeframes given by the arterial and venous compartments. Consequently, 2,3-BPG concentration is quasistationary and the nonlinear feedback effects of 2,3-BPG inhibition of PFK and HK that decline in the venous phase (coupled with a slight increase of MgATP at the same time) explains the observed increase of glycolytic flux in the venous phase (see e.g. Table S6 and Table 4).

Table 4
Distribution of hemoglobin species in late arterial and venous phase

Species	Arterial	Venous
Hb-ATP	2.8%	2.7%
Hb-MgATP	2.3%	1.8%
Hb-2,3-BPG	58.7%	76.5%
Hb-ADP	1.3%	1.1%
Hb-FBP	0.0%	0.0%
Hb-1,3-BPG	0.0%	0.0%
Free Hb	34.9%	17.9%

Total intracellular concentration of Hb is set to be 7.0 mM in the model.

5. Discussion

Erythrocyte metabolism provides an excellent example of a biological system operating on a multitude of time scales. The ensuing relaxation modes can be used as a tool to analyze complex models in order to reveal functional insights of the system near and at steady state. The location of a stable steady state in metabolite space depends on external conditions, e.g. the partial pressure of O_2. The main conclusions of this study are the following: 1) The periodic forcing of P_{O_2} is a primary driving force behind glycolytic flux changes in the circulation. 2) The exact geometry and time scale dispersal of fast and slow relaxation modes coupled with P_{O_2} transition frequency and amplitude bring about an overshoot phenomenon observed for both a

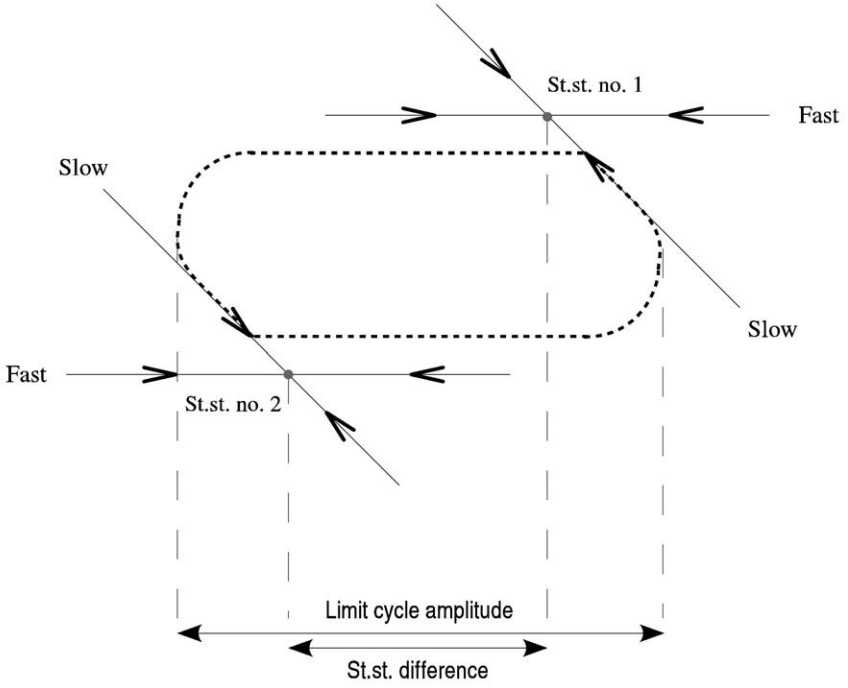

Fig. 5. Example of overshoot producing dynamics in a 2-dimensional phase plane. The location of the steady state (marked with a grey dot) depends on external parameters that display periodic transitions. Thus, two locations of the steady state are shown. The two non-perpendicular directions of relaxation – one fast and one slow – towards the steady state may be largely preserved upon the transition. Initially, the system is driven in the fast direction followed by relaxation along the slow direction. As the transition frequency is higher than the slow relaxation mode a limit cycle shown as a stippled curve emerges. As long as the eigenvectors are not perpendicular, concentration differences are greater (or smaller – as shown here in the vertical direction) on the limit cycle compared to the difference between steady state locations.

number of fluxes and metabolite concentrations. 3) The overshoots are augmented by the nonlinear effects of 2,3-BPG. The overshoot phenomenon, as illustrated in Fig. 5, is a general dynamical property of a driven system with a broad distribution of time scales. The requirements are 1) a periodic change of steady state location due to one or more oscillatory parameters and 2) that the directions of relaxation toward stationarity (approximated by eigenvectors) are not perpendicular. It is thus anticipated that the phenomenon is widespread in nature and must be taken into account both when studying externally forced systems and when applying a forcing onto such systems.

The predicted overshoots are expected to be hard to detect experimentally *in vivo* due to the fast Hb and Mg^{2+} binding reactions. However, the overshoots displayed by Mg^{2+}, ATP, and 2,3-BPG may have an important impact on erythrocyte secondary metabolism. Mg^{2+} and ATP are important cofactors and regulators of numerous reactions in the cell and Mg^{2+} is believed to regulate membrane stability [7,18,19]. 2,3-BPG is of central importance to hemoglobin function and glycolytic flux changes. The model predicts that total 2,3-BPG is at a quasi-steady state. In the arterial phase most 2,3-BPG is free or bound to Mg^{2+}. Free 2,3-BPG inhibits HK, PFK, and Ald. In the venous phase most is bound to Hb causing a rise in Mg^{2+} and a decline in enzyme inhibition. Also, the predictions of the arterio-venous concentration ratios could provide a switch mechanism to trigger or augment the secondary oxygenation dependent functions within the erythrocyte (transport activities [20], structural changes [21,22], membrane fluidity etc.).

As is seen, it is paramount to take the dynamics of a system into account in order to obtain a faithful representation of the system at hand. Determination of intracellular fluxes or concentrations of metabolites is (as far as we know) always carried out relatively long time (on the order of ~30 min to several hours) after withdrawal of sample blood (see [9,23] and references herein). This is usually done to ensure *steady state* conditions. Our results indicate that even longer time is required. In modern time NMR-studies (e.g. [8,16,24–26]) erythrocytes following removal of buffy coat are incubated up to several hours before measurement. The findings of the present study indicate that standard experimental procedures and steady state approximations may be unable to capture a number of important features of the erythrocyte system under the physiological conditions of arterio-venous oxygenation changes in the circulation.

5.1. cdB3 involvement

In the literature, the oxygen-dependent modulation of erythrocyte metabolism is assumed to be a result primarily of the interplay between Hb and cdB3 [7,8,27–31]. This study shows that glycolytic oscillations are able to occur without cdB3 involvement, albeit at this state of investigation our model cannot explain all the experimentally reported differences between oxy- and deoxygenated erythrocytes at steady state.

The cytoplasmatic domain of Band3 (cdB3) is a plausible effector on erythrocyte metabolism. Recent evidence [27,28,32] suggests that cdB3 is able to bind PFK, ALD, GAPDH, and Hb at the membrane and thereby initiate the formation of a glycolytic enzyme complex, which is expected to inhibit catalytic activities completely [29]. In a separate series of *in silico* experiments, we also included cdB3 binding to Ald, PFK, GAPDH, Hb_d, and Hb_o (data not shown) using a set of association constants used in an erythrocyte model by Kinoshita et al. [33]. The calculations showed even higher shifts of arterio-venous ratios both on the limit cycle and between the two steady states and we observed increased overshoots. However, with the cdB3 inclusion the free concentrations of ALD, PFK, and GAPDH became so low that it must be concluded that direct use of the published association constants of cdB3-bindings [33–36] must be wrong (see Table S2 in the SI). (True association constants depends heavily on ionic strength and local pH).

5.2. Model limitations

The most important limitation of our model and all other models of erythrocyte metabolism is the lack of detailed implementations of MgATP, NADH and NADPH/GSH consuming processes. All existing erythrocyte models [9,23,33,37,38] handle such processes by linear first order reactions with a generalized rate constant. Hence, the supply is modelled in detail, but models of the demand for these important cofactors are inadequate. For instance, metabolic control analysis reveal that the ATPase and the “spontaneous” oxidation reaction of GSH exert almost exclusive control of the flux through glycolytic and PPP, respectively [39]. In other organisms, for instance in *Escherichia coli*, glycolytic flux is controlled by the demand of ATP as well [40]. Metabolic models have to reflect the supply and demand of the relevant species (just as economical models have to account for incomes and expenditures) in order to hint useful answers to physiological questions.

The kinetic model developed by Mulquiney and Kuchel is a huge model comprised of many parameters and biochemical details. Thus, the model may contain considerable errors and may be shown to fit experimental data using a different set of parameters. It is difficult to assess to what extent the dynamic properties would have differed with other (hypothetical) sets of consistent parameter values. However, it seems reasonable to assume that the set of parameter values that fits the experimental data best also reflects true dynamical properties of the metabolic network *in vivo*.

In the context of circulating erythrocytes, the limitations imposed by the simplistic hemoglobin rate expression and the forcing model are not important, as the purpose of the model is not to be fully accountable of quantitative details (virtually impossible), but to display important flux and metabolite changes in the course of blood-stream traversal.

Limitations of our model include the lack of proper implementations of volume and pH changes. As noted in the ‘Methods section’, the minor pH changes at resting conditions only have a small degree of influence on metabolism. Volume changes are known to occur in erythrocytes because of the chloride shift. The retention of negative charge causes the erythrocytes to swell around 3% in the venous phase [13]. The presented model assumes a constant intracellular volume. However, a 3% change of volume will not affect the calculations of this study significantly.

New experimental research suggest that ATP is released upon hypoxic conditions [41–44]. The corresponding changes in ATP level seems to be low compared with the intracellular concentration. As the time scale of adenine turnover seems to be around two weeks [9] in the presence of glucose we have chosen to set the total nucleotide content constant in this study.

Validation of the model and the results of this study would require measurements of erythrocytes moving between chemically well-defined arterial and venous compartments of a chemical reactor. A verification of the long relaxation times of 2,3-BPG production could be carried out by simultaneous measurements of glucose uptake rate and the total concentration of intracellular 2,3-BPG from freshly drawn erythrocytes in venous and arterial blood by NMR.

6. Conclusion

In this study we have shown that the respiratory forcing of erythrocyte metabolism results in a) glycolytic flux oscillations and b) overshoots of central metabolites. This behavior can be explained by the fixed period and amplitude of oxygen exchange during circulation coupled with the slow modes of glycolysis, metabolite transport and 2,3-BPG production. Systems with dispersed time scale distributions coupled to periodic changes in a steady state location may often produce a dynamic behavior equivalent to the observed behavior of erythrocyte metabolism forced by respiration.

Acknowledgements

This work was supported by the European Union through the Network of Excellence BioSim, Contract No. LSHB-CT-2004-005137 and by the European Science Foundation FuncDyn Programme.

Appendix A. Supplementary data

Supplementary data associated with this article can be found, in the online version, at doi:10.1016/j.bpc.2008.12.008.

References

[1] R. Heinrich, S. Schuster, The Regulation of Cellular systems, Chapman & Hall (ITP), 1996.
[2] J. Liao, E. Lightfoot Jr., Extending the quasi-steady state concept to analysis of metabolic networks, J. Theor. Biol. 126 (1987) 253–273.
[3] I. Messana, M. Orlando, L. Cassiano, L. Pennacchietti, C. Zuppi, M. Castagnola, B. Giardina, Human erythrocyte metabolism is modulated by the O_2-linked transition of hemoglobin, FEBS 390 (1996) 25–28.
[4] N. Hamasaki, T. Asakura, S. Minakami, Effect of oxygen tension on glycolysis in human erythrocytes, J. Biochem. (Tokyo) 68 (2) (1970) 157–161.
[5] I. Rapoport, H. Berger, S.M. Rapoport, Response of the glycolysis of human erythrocytes to the transition from the oxygenated to the deoxygenated state at constant intracellular pH, Biochim. Biophys. Acta 428 (1976) 193–204.
[6] J.R. Murphy, Erythrocyte metabolism II. Glucose metabolism and pathways, J. Lab. Clin. Med. 55 (1960) 286–302.
[7] N.N. Barvitenko, N.C. Adragna, R.E. Weber, Erythrocyte signal transduction pathways, their oxygenation dependence and functional significance, Cell. Physiol. Biochem. 15 (2005) 1–18.
[8] A. Galtieri, E. Tellone, L. Romano, F. Misiti, E. Bellocco, S. Ficarra, A. Russo, D. Di Rosa, M. Castagnola, B. Giardina, I. Messana, Band 3 protein function in human erythrocytes: effect of oxygenation–deoxygenation, Biochim. Biophys. Acta 1564 (2002) 214–218.
[9] P.J. Mulquiney, P.W. Kuchel, Model of 2,3-bisphosphoglycerate metabolism in the human erythrocyte based on detailed enzyme kinetic equations: equations and parameter refinement, Biochem. J. 342 (1999) 581–596.
[10] P. Mulquiney, P. Kuchel, Modelling Metabolism with Mathematica Analysis of Human Erythrocyte, CRC Press Inc., 2003.
[11] R. Dash, J. Bassingthwaighte, Blood HbO_2 and $HbCO_2$ dissociation curves at varied O_2, CO_2, pH, 2,3-DPG and temperature levels, Ann. Biomed. Eng. 32 (12) (2004) 1676–1693.
[12] F. Hynne, P. Graae Sørensen, T. Møller, Complete optimization of models of the Belousov–Zhabotinsky reaction at a Hopf bifurcation, J. Chem. Phys. 98 (1) (1993) 219–230.
[13] W. Ganong, Review of Medical Physiology, 22.th ed., McGraw-Hill Companies, 2005.
[14] Y. Enoki, S. Tomita, N. Maeda, M. Kawase, T. Okuda, A simple method for determination of red cell intracellular pH, Nippon Seirigaku Zasshi 34 (11) (1972) 761–762.
[15] J. Freedman, J. Hoffman, Ionic and osmotic equilibria of human red blood cells treated with nystatin. J. Gen. Physiol. 74 (2) (1979) 157–185.
[16] R.J. Labotka, Measurement of intracellular pH and deoxyhemoglobin concentration in deoxygenated erythrocytes by phosphorus-31 nuclear magnetic resonance, Biochemistry 23 (23) (1984) 5549–5555.
[17] S. Cohen, A. Hindmarsh, CVODE user guide, Lawrance Livermore National Laboratory report UCRL-MA-118618.
[18] G. Beaven, J. Parmar, G. Nash, B. Bennett, W. Gratzer, Effect of magnesium ions on red cell membrane properties, J. Membr. Biol. 118 (3) (1990) 251–257.
[19] S. Page, M. Salem, M. Laughlin, Intracellular Mg2+ regulates ADP phosphorylation and adenine nucleotide synthesis in human erythrocytes, Am. J. Physiol. (Endocrinol. Metab.) 274 (1998) 920–927.
[20] J. Gibson, A. Cossins, J. Ellory, Oxygen-sensitive membrane transporters in vertebrate red cells, J. Exp. Biol. 203 (2000) 1395–1407.
[21] S. Tuvia, S. Levin, R. Korenstein, Oxygenation–deoxygenation cycle of erythrocytes modulates submicron cell membrane fluctuations, Biophys. J. 63 (1992) 599–602.
[22] A. Barbul, Y. Zipser, A. Nachles, R. Korenstein, Deoxygenation and elevation of intracellular magnesium induce tyrosine phosphorylation of band 3 in human erythrocytes, FEBS Lett. 455 (1999) 87–91.
[23] A. Joshi, B.O. Palsson, Metabolic dynamics in the human red cell. Part I – A comprehensive kinetic model, J. Theor. Biol. 141 (1990) 515–528.
[24] H.A. Berthon, W.A. Bubb, P.W. Kuchel, 13C n.m.r. isotopomer and computer-simulation studies of the non-oxidative pentose phosphate pathway of human erythrocytes, Biochem. J. 296 (Pt 2) (1993) 379–387.
[25] A. Petersen, S. Risom-Kristensen, J.P. Jacobsen, M. Horder, ^{31}P-NMR measurements of ATP, ADP, 2,3-diphosphoglycerate and Mg^{2+} in human erythrocytes, Biochim. Biophys. Acta 1035 (1990) 169–174.
[26] I. Messana, F. Misiti, S. el Sherbini, B. Giardina, M. Castagnola, Quantitative determination of the main glucose metabolic fluxes in human erythrocytes by 13C- and 1H-MR spectroscopy, J. Biochem. Biophys. Methods 39 (1999) 63–84.
[27] R.E. Weber, W. Voelter, A. Fago, H. Echner, E. Campanella, P.S. Low, Modulation of red cell glycolysis: interactions between vertebrate hemoglobin and cytoplasmic domains of band 3 red cell membrane proteins, Am. J. Physiol., Regul. Integr. Comp. Physiol. 287 (2004) 454–464.
[28] M.E. Campanella, H. Chu, P.S. Low, Assembly and regulation of a glycolytic enzyme complex on the human erythrocyte membrane, PNAS 102 (2005) 2402–2407.
[29] P.S. Low, P. Rathinavelu, M.L. Harrison, Regulation of glycolysis via reversible enzyme binding to the membrane protein, Band 3, J. Biol. Chem. 268 (1993) 14627–14631.
[30] P.S. Low, Structure and function of the cytoplasmic domain of band 3: center of erythrocyte membrane-peripheral protein interactions, Biochim. Biophys. Acta 864 (1986) 145–167.
[31] P.S. Low, D.P. Allen, T.F. Zioncheck, P. Chari, B.M. Willardson, R.L. Geahlen, M.L. Harrison, Tyrosine phosphorylation of band 3 inhibits peripheral protein binding, J. Biol. Chem. 262 (10) (1987) 4592–4596.
[32] B. von Rückmann, D. Schubert, The complex of band 3 protein of the human erythrocyte membrane and glyceraldehyde-3-phosphate dehydrogenase: stoichiometry and competition by aldolase, Biochim. Biophys. Acta 1559 (1) (2002) 43–55.
[33] A. Kinoshita, K. Tsukada, T. Soga, T. Hishiki, Y. Ueno, Y. Nakayama, M. Tomita, M. Suematsu, Roles of hemoglobin allostery in hypoxia-induced metabolic alterations in erythrocytes: simulation and its verification by metabolome analysis. J. Biol. Chem. 282 (14) (2007) 10731–10741.
[34] G.E. Kelley, D.J. Winzor, Quantitative characterization of the interactions of aldolase and glyceraldehyde-3-phosphate dehydrogenase with erythrocyte membranes. Biochim. Biophys. Acta 778 (1) (1984) 67–73.
[35] J.A. Walder, R. Chatterjee, T.L. Steck, P.S. Low, G.F. Musso, E.T. Kaiser, P.H. Rogers, A. Arnone, The interaction of hemoglobin with the cytoplasmic domain of band 3 of the human erythrocyte membrane, J. Biol. Chem. 259 (16) (1984) 10238–10246.
[36] J.D. Jenkins, D.P. Madden, T.L. Steck, Association of phosphofructokinase and aldolase with the membrane of the intact erythrocyte. J. Biol. Chem. 259 (15) (1984) 9374–9378.
[37] T.A. Rapoport, R. Heinrich, Mathematical analysis of multienzyme systems. I. Modelling of the glycolysis of human erythrocytes, BioSystems 7 (1975) 120–129.
[38] T. Ni, M.A. Savageau, Model assessment and refining using strategies from biochemical systems theory: application to metabolism in human red blood cells, J. Theor. Biol. 179 (1996) 329–368.
[39] P.J. Mulquiney, P.W. Kuchel, Model of 2,3-bisphosphoglycerate metabolism in the human erythrocyte based on detailed enzyme kinetic equations: computer simulation and metabolic control analysis, Biochem. J. 342 (1999) 597–604.
[40] B.J. Koebmann, H.V. Westerhoff, J.L. Snoep, D. Nilsson, P.R. Jensen, The glycolytic flux in *Escherichia coli* is controlled by the demand for ATP, J. Bacteriol. 184 (14) (2002) 3909–3916.
[41] M. Ellsworth, Red blood cell-derived ATP as a regulator of skeletal muscle perfusion, Med. Sci. Sports Exerc. 36 (1) (2003) 35–41.
[42] M. Farias III, M.W. Gorman, M.V. Savage, E.O. Feigl, Plasma ATP during exercise: possible role in regulation of coronary blood flow, Am. J. Physiol., Heart Circ. Physiol. 288 (2004) 1586–1590.
[43] R.S. Sprague, A.H. Stephenson, M. Ellsworth, C. Keller, A.J. Lonigro, Impaired release of ATP from RBCs of humans with primary pulmonary hypertension, Exp. Biol. Med. 226 (5) (2001) 434–439.
[44] J. Gonzalez-Alonso, D.B. Olsen, B. Saltin, Erythrocyte and the regulation of human skeletal muscle blood flow and oxygen delivery. Role of circulating ATP, Circ. Res. 91 (2002) 1046–1055.
[45] W. Boron, E. Boulpaep, 2003, Medical Physiology, Elsevier (Saunders).